



## OPEN ACCESS

## EDITED BY

Carmen G. Feijoo,  
Andres Bello University, Chile

## REVIEWED BY

Shuang Zhang,  
Guangdong Ocean University, China  
Zhigang Zhou,  
Feed Research Institute (CAAS), China  
Yuliang Wei,  
Yellow Sea Fisheries Research  
Institute, Chinese Academy of Fishery  
Sciences, China

## \*CORRESPONDENCE

Yanjiao Zhang  
yanjiaozhang@ouc.edu.cn  
Junming Deng  
djunming@163.com

## SPECIALTY SECTION

This article was submitted to  
Comparative Immunology,  
a section of the journal  
Frontiers in Immunology

RECEIVED 05 July 2022

ACCEPTED 15 August 2022

PUBLISHED 08 September 2022

## CITATION

Chen Z, Huang D, Yongyut P, Li G,  
Esteban MÁ, Jintasataporn O, Deng J,  
Zhang W, Ai Q, Mai K and Zhang Y  
(2022) Vitamin D<sub>3</sub> deficiency induced  
intestinal inflammatory response of  
turbot through nuclear factor- $\kappa$ B/  
inflammasome pathway, accompanied  
by the mutually exclusive apoptosis  
and autophagy.  
*Front. Immunol.* 13:986593.  
doi: 10.3389/fimmu.2022.986593

## COPYRIGHT

© 2022 Chen, Huang, Yongyut, Li,  
Esteban, Jintasataporn, Deng, Zhang, Ai,  
Mai and Zhang. This is an open-access  
article distributed under the terms of  
the [Creative Commons Attribution  
License \(CC BY\)](https://creativecommons.org/licenses/by/4.0/). The use, distribution  
or reproduction in other forums is  
permitted, provided the original  
author(s) and the copyright owner(s)  
are credited and that the original  
publication in this journal is cited, in  
accordance with accepted academic  
practice. No use, distribution or  
reproduction is permitted which does  
not comply with these terms.

# Vitamin D<sub>3</sub> deficiency induced intestinal inflammatory response of turbot through nuclear factor- $\kappa$ B/inflammasome pathway, accompanied by the mutually exclusive apoptosis and autophagy

Zhichu Chen<sup>1,2</sup>, Dong Huang<sup>1</sup>, Prakaiwan Yongyut<sup>3</sup>,  
Guangbin Li<sup>4</sup>, María Ángeles Esteban<sup>2</sup>, Orapint Jintasataporn<sup>3</sup>,  
Junming Deng<sup>4\*</sup>, Wenbing Zhang<sup>1</sup>, Qinghui Ai<sup>1</sup>,  
Kangsen Mai<sup>1</sup> and Yanjiao Zhang<sup>1\*</sup>

<sup>1</sup>The Key Laboratory of Aquaculture Nutrition and Feed (Ministry of Agriculture) and the Key Laboratory of Mariculture (Ministry of Education), Ocean University of China, Qingdao, China,

<sup>2</sup>Fish Innate Immune System Group, Department of Cell Biology and Histology, Faculty of Biology, University of Murcia, Murcia, Spain, <sup>3</sup>Department of Aquaculture, Faculty of Fisheries, Kasetsart University, Bangkok, Thailand, <sup>4</sup>Laboratory of Aquatic Animal Nutrition and Feed, Fisheries College, Guangdong Ocean University, Zhanjiang, China

Vitamin D<sub>3</sub> (VD<sub>3</sub>) participated widely in the nuclear factor- $\kappa$ B (NF- $\kappa$ B)-mediated inflammation, apoptosis, and autophagy through the vitamin D receptor (VDR). However, the molecular mechanisms remain not understood in teleost. The present study investigated the functions of VD<sub>3</sub>/VDR on intestinal inflammation, autophagy, and apoptosis of turbot *in vivo* and *in vitro*. Triple replicates of 30 fish were fed with each of three diets with graded levels of 32.0 (D<sub>0</sub>), 1012.6 (D<sub>1</sub>), and 3978.2 (D<sub>2</sub>) IU/kg VD<sub>3</sub>. Obvious intestinal enteritis was observed in the D<sub>0</sub> group and followed with dysfunction of intestinal mucosal barriers. The intestinal inflammatory response induced by VD<sub>3</sub> deficiency was regulated by the NF- $\kappa$ B/inflammasome signalling. The promotion of intestinal apoptosis and suppression of intestinal autophagy were also observed in the D<sub>0</sub> group. Similarly, VD<sub>3</sub> deficiency *in vitro* induced more intense inflammation regulated by NF- $\kappa$ B/inflammasome signalling. The mutually exclusive apoptosis and autophagy were also observed in the group without 1,25(OH)<sub>2</sub>D<sub>3</sub> *in vitro*, accompanied by similar changes in apoptosis and autophagy increased apoptosis. The gene expression of VDRs was significantly increased with the increasing VD<sub>3</sub> supplementation both *in vivo* and *in vitro*. Moreover, VDR knockdown in turbot resulted in intestinal inflammation, and this process relied on the activation of inflammasome mediated by NF- $\kappa$ B signalling. Simultaneously, intestinal apoptosis was promoted, whereas intestinal autophagy was inhibited. In conclusion, VD<sub>3</sub> deficiency could induce intestinal inflammation *via* activation of the NF- $\kappa$ B/inflammasome pathway,

intestinal apoptosis, and autophagy formed a mutually exclusive relation in teleost. And VDR is the critical molecule in those processes.

#### KEYWORDS

vitamin D<sub>3</sub>, vitamin D<sub>3</sub> receptor, NF-κB, inflammasome, inflammation, apoptosis, autophagy

## 1 Introduction

In fish, the intestine is a major immune organ that provides a tight barrier against pathogenic infections and coexists with many commensal organisms while absorbing and metabolizing nutrients (1, 2). The pathological process of enteritis in fish is closely associated with dysfunction of intestinal mucosal barriers, including the overexpression of pro-inflammatory cytokines, abnormal tight junction protein assembly, and decreased mucin secretion (3–6). In a variety of nutrients that can enhance the intestinal health of aquatic animals, it has been widely proven that dietary vitamin D<sub>3</sub> (VD<sub>3</sub>) could improve intestinal digestion and utilization of nutrients, alleviating intestinal inflammation (5, 7, 8). However, there is no existent for the autonomous synthesis of VD<sub>3</sub> in fish (9). Generally, fish need vitamin D<sub>3</sub> supplements through feed and then metabolize it into 1,25(OH)<sub>2</sub>D<sub>3</sub> and exert biological activity.

In mammals, VD<sub>3</sub> signalling through its nuclear vitamin D receptor (VDR) has emerged as a key immune system modulator. Decreased serum 1,25(OH)<sub>2</sub>D<sub>3</sub> levels or VD<sub>3</sub> deficiency has been linked to human intestinal diseases, such as inflammatory bowel diseases and short bowel syndrome (10–12). In the development of intestinal inflammation, there was an important role of VD<sub>3</sub> and VDR in maintaining intestinal barrier function and innate antibacterial immunity. Such as, in

Caco-2 cells, 1,25(OH)<sub>2</sub>D<sub>3</sub> increased junction protein expression and intestinal transepithelial electric resistance and preserved the integrity of tight junctions in the presence of dextran sulfate sodium (DSS) (13). Administration of 1,25(OH)<sub>2</sub>D<sub>3</sub> downregulates cadherin-17 but upregulates tight junction proteins (claudin 2 and 12) expression in the intestine of calbindin-D<sub>9k</sub> null mutant mice (14). Furthermore, VDR deletion in intestinal epithelial cells leads to the decreased expression of claudin 2 and 12 in the intestine of mice and intestinal cell line Caco-2 (15). In addition, the activation of the NF-κB pathway by VD<sub>3</sub> was also observed in juvenile Chinese mitten crabs (*Eriocheir sinensis*) that VD<sub>3</sub> might improve intestinal immunity via the VDR/TLR/MyD88/NF-κB pathway (5). However, whether VD<sub>3</sub>/VDR mediated intestinal barrier function and NF-κB signalling pathway involved in regulating intestinal inflammation is not comprehensively understood in the teleost.

Excess cytokine production by activated intraepithelial lymphocytes and other immune cells can induce apoptosis directly by suppressing anti-apoptotic signals in the epithelium (16–18). Additionally, autophagy plays a key role in the prevention of intestinal inflammation, impaired autophagy exhibit exacerbated colitis induced by DSS in different autophagy-deficient mice models (19–22), and the activation of autophagy suppressed intestinal inflammation in experimental models of colitis and Crohn's disease (23–25). Moreover, VD<sub>3</sub> has been regarded as an opponent of colorectal cancer by inhibiting epithelial cell apoptosis, while an increased number of apoptotic cells was observed in the small intestine of VDR-deficient mice (26–28). Furthermore, apoptosis and autophagy balance is critical for maintaining the normal functions of the intestine (27). Previous studies have shown that the regulation of intestinal epithelial VDR depends on the autophagy pathway of autophagy related 16 like protein 1 (ATG16L1), while ATG16L1 was regulated by activated caspase-3 in the process of apoptosis (29–31). A similar result in abalone showed that dietary VD<sub>3</sub> can inhibit apoptosis and produce autophagy simultaneously (32). However, the regulation of VD<sub>3</sub>/VDR in the interaction of intestinal apoptosis and autophagy in teleost is still unknown.

Turbot (*Scophthalmus maximus* L.) is cultured wildly in the world. In recent years, more and more attention has been paid to

**Abbreviations:** ACP, acid phosphatase; ALP, alkaline phosphatase; ANOVA, one-way analysis of variance; ATG16L1, Autophagy Related 16 Like 1; BAK, BCL2 Antagonist/Killer; BAX, BCL2 Associated X, Apoptosis Regulator; BCA, bicinchoninic acid; BCL2, BCL2 Apoptosis Regulator; BSA, Bovine Serum Albumin; CASP3, Caspase 3; CLDN4, Claudin 4; DSS, dextran sulfate sodium; GAPDH, Glyceraldehyde-3-phosphate dehydrogenase; H&E, hematoxylin and eosin; HBSS, Hank's Balanced Salt Solution; IFNG, Interferon Gamma; IL10, Interleukin 10; IL1B, Interleukin 1 Beta; IL8, Interleukin 8; Junctional adhesion molecule 1; LYZ, lysozyme; MAP1LC3B, Microtubule Associated Protein 1 Light Chain 3 Beta; MUC2&18, Mucin 2&18; RNAi, RNA interference; RPSD, RNA polymerase II subunit D; SD, standard deviation; TGFβ1, Transforming Growth Factor Beta 1; TNF, Tumor Necrosis Factor; TRIC, Tricellulin; JAM1, Junctional adhesion molecule 1; VD<sub>3</sub>, Vitamin D<sub>3</sub>; VDRA&B, Vitamin D Receptor A&B; ZO1, Zonula Occludens 1.

regulating intestinal health through nutritional strategy in the healthy cultivation of fish. Therefore, the present study aimed to evaluate the role of VD<sub>3</sub> in regulating intestinal inflammation and the relationship between intestinal apoptosis and autophagy in turbot.

## 2 Materials and methods

### 2.1 Experiment 1: Diets, fish husbandry, and sampling of VD<sub>3</sub> treatments *in vivo*

As shown in Table 1, three isonitrogenous and isolipidic experimental diets were formulated to contain approximately 50% crude protein and 10% crude lipid. The basal diet used casein (vitamin free), gelatine, and crystalline amino acid as the primary protein sources, while fish oil, soya bean oil, and soya bean lecithin were used as dietary lipid sources. VD<sub>3</sub> (V8070, Solarbio, China) was added to the basal diet to provide graded

concentrations of 0 (D<sub>0</sub>), 1000 (D<sub>1</sub>), and 4000 (D<sub>2</sub>) IU/kg VD<sub>3</sub>. The measured values of VD<sub>3</sub> concentration were determined by the high-performance liquid chromatography (HPLC) method as described previously (33), which were 32 (D<sub>0</sub>), 1012.60 (D<sub>1</sub>), and 3978.2 (D<sub>2</sub>) IU/kg. Diets were extruded with an experimental single-screw feed mill (Yihe, China) in the form of 3 mm diameter pellets and dried for 12 h in a ventilated oven at 50°C. All the experimental diets were stored at -20°C until use.

Disease-free juvenile turbots were purchased from a local farm in Weihai, Shandong Province, China. Before the start of the feeding trial, the fish were maintained for two weeks to acclimate to the experimental conditions. A commercial diet (Surgreen, China) was fed during the acclimation, which is specially formulated for the nutritional requirements of the turbot. The fish were then fasted for 24 h and weighed. A total of 270 fish (12.17 g initial body weight) were randomly assigned to 9 fiberglass tanks (300 L, 30 fish per tank) connected to an indoor flow-through water system. Triplicate tanks of fish were

TABLE 1 Formulation and proximate composition of the experimental diets (% dry matter).

Ingredients	Diets		
	D0	D1	D2
Casein (vitamin free)	37.20	37.20	37.20
Gelatin	9.30	9.30	9.30
Crystalline amino acid <sup>a</sup>	5.60	5.60	5.60
Fish oil	5.50	5.50	5.50
Soya oil	4.10	4.10	4.10
Soybean lecithin	1.00	1.00	1.00
Choline chloride	0.30	0.30	0.30
Ca(H <sub>2</sub> PO <sub>4</sub> ) <sub>2</sub> ·H <sub>2</sub> O	1.50	1.50	1.50
Ethoxyquin	0.05	0.05	0.05
Y <sub>2</sub> O <sub>3</sub>	0.10	0.10	0.10
Calcium propionate	0.10	0.10	0.10
Phagostimulant <sup>b</sup>	1.00	1.00	1.00
Dextrin	26.50	26.50	26.50
Microcrystalline cellulose	5.75	5.75	5.75
Mineral premix <sup>c</sup>	1.00	1.00	1.00
Vitamin premix <sup>d</sup>	1.00	1.00	1.00
Vitamin D <sub>3</sub> (add value, IU/kg)	0.00	1,000.00	4,000.00
<b>Proximate composition</b>			
Vitamin D <sub>3</sub> (measured value, IU/kg)	32.00	1,012.60	3,978.20
Moisture	9.83	9.21	10.09
Crude protein	50.29	50.14	50.11
Crude lipid	9.39	9.59	9.65
Ash	3.44	3.40	3.42

<sup>a</sup>Crystalline amino acid premix (g/100 g diet): arginine, 1.69; histidine, 0.55; isoleucine, 0.22; leucine, 0.14; lysine, 0.73; phenylalanine, 0.50; threonine, 0.61; valine, 0.13; alanine, 1.32; aspartic acid, 1.63; glycine, 1.62; serine, 0.42; cystine, 0.40; tyrosine, 0.10.

<sup>b</sup>Phagostimulant (g/kg diet): betaine, 4; DMPT, 2; threonine, 2; glycine, 1; inosine-5'-diphosphate trisodium salt, 1.

<sup>c</sup>Mineral premix (mg/kg diet): FeSO<sub>4</sub>·H<sub>2</sub>O, 80; ZnSO<sub>4</sub>·H<sub>2</sub>O, 50; CuSO<sub>4</sub>·5H<sub>2</sub>O, 10; MnSO<sub>4</sub>·H<sub>2</sub>O, 45; KI, 60; CoCl<sub>2</sub>·6H<sub>2</sub>O (1%), 50; Na<sub>2</sub>SeO<sub>3</sub> (1%), 20; MgSO<sub>4</sub>·7H<sub>2</sub>O, 1200; zeolite, 8485.

<sup>d</sup>Vitamin premix (mg/kg diet): retinyl acetate, 32; DL- $\alpha$ -tocopherol acetate, 240; vitamin K<sub>3</sub>, 10; thiamin, 25; riboflavin (80%), 45; pyridoxine hydrochloride, 20; vitamin B<sub>12</sub> (1%), 10; Lascorbyl-2-monophosphate-Na (35%), 2000; calcium pantothenate, 60; nicotinic acid, 200; inositol, 800; biotin (2%), 60; folic acid, 20; cellulose, 6478.

fed with each experimental feed to apparent satiation twice daily for 12 weeks. During the feeding period, water temperature ranged from 15°C to 18°C; salinity 30-33‰; and dissolved oxygen higher than 7.0 mg/L.

Three fish were selected randomly from each tank for the sampling. All fish were anesthetized with eugenol (1:10000, Shanghai Reagent Corp, China) before handling. The intestinal tissue samples for the analysis of enzymes activities, DNA laddering, gene expression, and western blot were frozen in liquid nitrogen, and the others for the analysis of histology were fixed in Bouin's fixative solution.

## 2.2 Experiment 2: Cell culture and sampling of VD<sub>3</sub> treatments *in vitro*

According to our previous study (34), the isolation and culture of primary intestinal epithelial cells were performed. Briefly, the starved turbot were anesthetized with eugenol (1:10000, Shanghai Reagent Corp, China), wiped, and disinfected with 75% ethanol. Then the intestine tissue was dissected and rinsed repeatedly with the solution of Hank's Balanced Salt Solution (HBSS) containing penicillin-streptomycin (Thermo Fisher Scientific, USA). About 1 mm<sup>3</sup> of intestinal tissues were dissociated with collagenase and dispase (Thermo Fisher Scientific, USA) for 15 to 20 min. The enzyme solution was washed several times with L-15 medium (L5520, Sigma, USA), and the supernatants were collected and centrifuged for 5 min at 1000 rpm to obtain intestinal epithelial cells suspended in the supernatants.

The intestinal epithelial cells were seeded into 6-well plates at a density of 1.0×10<sup>6</sup> cells/mL with a modified L-15 medium (L5520, Sigma, USA) containing 5% fetal bovine serum (FBS, Biological Industries, Israel), 10 ng/mL epidermal growth factor (Sigma, USA), 0.2% insulin transferrin-selenium-sodium pyruvate (Thermo Fisher Scientific, USA), antifungal, and antibacterial substances at 23°C in an incubator (CO<sub>2</sub>-free). After the cells adhered to the well for 24 h, the cells were treated with fresh medium together with 0, 1, 10, and 50 nM 1,25(OH)<sub>2</sub>D<sub>3</sub> (HY-10002, Med Chem Express, USA). After 1,25(OH)<sub>2</sub>D<sub>3</sub> treatments for 24 h, the cell lysates were subjected to RNA and protein extraction, while the cell climbing slides were fixed with 4% paraformaldehyde for TUNEL assay and MAP1LC3B immunofluorescence.

## 2.3 Experiment 3: RNA interference of VDRs *in vivo* and sampling

Three pairs of VDR-specific siRNAs and scrambled siRNA for negative control (NC siRNA) set up through BLOCK-iT<sup>TM</sup> RNAi Express are shown in Table 2 and Figure S, and synthesized by T7 RNAi Transcription Kit (TR102, Vazyme,

China) according to the instructions. Seven groups of 9 turbot acclimating to an indoor flow-through water system were injected with VDR-specific siRNAs (1 µg/g) and NC siRNA (1 µg/g), and the intestinal tissues were drawn to analyze the gene expression of VDRA&B gene expression after 24 h. Three turbot were mixed together to make a sample. And the most effective siRNA of VDRA&B was selected for the formal experiment.

The formal *RNA interference* (RNAi) experiment lasted for two days. The body weight of the fish decided the dose of siRNA (1 µg/g). Five groups of 9 turbot were injected with equal volume (100 µl) of PBS, PBS, NC siRNA, VDRA siRNA, and VDRB siRNA on the first day, respectively. After 24 h, they continued to be injected with the same contents as the first day. In addition to the first group still injected with PBS, the last four groups were injected with lipopolysaccharides (LPS) at the rate of 2.5 µg/g body weight. They were defined as PBS, LPS, NC siRNA+LPS, VDRA siRNA+LPS, and VDRB siRNA+LPS group. The turbot were anesthetized by eugenol (1:10000, Shanghai Reagent Corp, China) and had their intestinal tissue taken for qRT-PCR and western blot.

## 2.4 Chemical analysis of diets

Standard methods (AOAC, 1995) were used for analyzing experimental diets. Moisture content was determined gravimetrically to constant weight in an oven at 105°C. Crude protein was determined by the Kjeldahl method using Kjeltec 2300 (Foss, Denmark) using boric acid to trap released ammonia. Crude lipid was determined by petroleum ether extraction using Soxhlet Extraction System B-811 (Buchi, Switzerland). Ash was determined by combustion at 550°C.

## 2.5 Intestinal histology

After being fixed in Bouin's fixative solution for 24 h, the intestinal samples were transferred to 70% ethanol and embedded in paraffin after dehydration. Paraffin sections of 5 µm were cut and stained with hematoxylin and eosin (H&E,

TABLE 2 siRNA sequences.

	Sequence
VDRA siRNA 1	CAATGTTTCTAGATGTTTA
VDRA siRNA 2	GTTCAAAGATTGAAATCAA
VDRA siRNA 3	GCTGTGGTGTAGCAAGTTA
VDRB siRNA 1	GGACCTTCATATAATACAA
VDRB siRNA 2	GGTTGATGATTTTGACTAA
VDRB siRNA 3	GGATGTACACCATACTCTA
NC siRNA	GCTGACCCTGAAGTTCATC

G1120, Solarbio, China) according to the manufacturer's protocol. The slides were examined under a light microscope (BX43F, Olympus, Japan) equipped with a digital microscope camera (DP72, Olympus, Japan) for image acquisition.

## 2.6 Intestine-related enzyme activities

For the analysis of intestinal alkaline phosphatase (ALP), acid phosphatase (ACP), and lysozyme (LYZ) activities, the intestinal samples were homogenized in ice-cold physiological saline solution (1:9) and centrifuged at 2500 g for 10 min at 4°C. The relevant intestinal enzyme activities were then determined with supernatants, whose protein concentrations were measured by the bicinchoninic acid (BCA) protein analysis kit (P0012, Beyotime, China). The activities of ALP (A059-2), ACP (A060-2), and LYZ (A050-1) were quantified using the commercial kits according to the manufacturer's protocol (Jiancheng Bioengineering Institute, China).

## 2.7 DNA fragmentation assay

Briefly, 5 mg intestinal tissues were homogenized in liquid nitrogen and then mixed with 0.5 ml DNA extraction lysis buffer (pH 8.0) containing 50 mM Tris-HCl (Solarbio, China), 25 mM EDTA (Solarbio, China), 100 mM NaCl (Macklin, China), 1% Triton X-100 (Solarbio, China), and 0.5 mg/ml Protease K (Solarbio, China). The lysates were incubated overnight at 50°C with gentle shaking and then mixed with an equal volume of phenol-chloroform-isoamyl alcohol (25:24:1) (Solarbio, China). After being precipitated with 5 M ammonium acetate (Solarbio, China) and absolute ethanol (Sangon, China), the DNA precipitations were washed three times with 0.6 ml 70% ethanol and air-dried at room temperature (RT). The DNA precipitations were dissolved with Tris-EDTA buffer (Solarbio, China) containing 100 µg/ml RNase A (Solarbio, China) and incubated at 30°C for 30 min. Approximately 5 µg of DNA samples were electrophoresed (100 V) on a 2% agarose gel and were visualized with Gel-Red (TransGen Biotech, China) and recorded under UV light with an Odyssey Infrared Imaging System (Li-Cor Bioscience, USA). Trans2K<sup>®</sup> Plus DNA Marker (BM111, TransGen, China) of nuclei acid was used as the reference. The evaluation of DNA fragmentation was determined according to Yuan et al. (35). The density of the 180 to 200 bp DNA band was quantified using ImageJ software (National Institutes of Health, USA), and the relative density was normalized to the D<sub>0</sub> group.

## 2.8 TUNEL, immunofluorescence, and photomicrograph

TMR (red) TUNEL Cell Apoptosis Detection Kit (G1502, Servicebio, China) was used to detect positive apoptotic nuclei of cell climbing slides. The cell climbing slides were dried and then incubated in the permeabilizing work solution for 20 min at RT. Rinse with PBS solution three times, each for 5 min. After the slices were slightly dried, the equilibration buffer was added to the tissues and incubated for 10 min at RT. After washing with PBS solution three times (5 min per time), the TUNEL reaction solution mixture (TDT enzyme, dUTP, and buffer at 1:5:50 ratio) was added to objective tissue placed in a flat wet box, incubated for 2 h at 37°C. 4',6-diamidino-2-phenylindole (DAPI) was used to stain the nucleus and washed out three times with PBS in a rocker device.

Immunofluorescence was used for detecting MAP1LC3B in climbing slides. The cell membrane rupture was conducted as mentioned above, and then the slides were incubated in 5% Bovine Serum Albumin (BSA) for 30 min at RT. MAP1LC3B antibody (AF5225, Beyotime, China) was added to the sections, and the slides were incubated overnight at 4°C. After being washed with PBS solution three times (5 min per time), the tissues were covered with the secondary antibody and incubated for 50 min at RT. The nucleus was stained by DAPI and washed three times with PBS.

The sections were observed under a fluorescence microscope, and images were collected. (DAPI UV excitation wavelength 330-380 nm, emission wavelength 420 nm, blue light emission; CY3 excitation wavelength 510-561 nm, emission wavelength 590 nm, red light emission).

## 2.9 RNA extraction and quantitative real-time PCR (qRT-PCR)

RNA was extracted from the intestinal samples with Trizol Reagent (Takara, Japan). The integrity of RNA was detected by electrophoresis on 1% denaturing agarose gel, and the concentration was detected with a Nano Drop<sup>®</sup>2000 spectrophotometer (Thermo Fisher Scientific, USA). A total of 1 µg RNA was reversely transcribed to cDNA with Evo M-MLV Mix Kit with gDNA Clean for qPCR [#AG11728, Accurate Biotechnology (Hunan) Co., Ltd., China].

The gene expression of VD<sub>3</sub> receptor A and B (*VDRA* & *B*), interleukin 1 beta (*IL1B*), interleukin 8 (*IL8*), tumor necrosis factor (*TNF*), and interferon gamma (*IFNG*), apoptosis-associated speck-like protein containing a caspase recruitment domain (*ASC*), transforming growth factor beta 1 (*TGFB1*), and

interleukin-10 (*IL 10*), B cell lymphoma 2 (*BCL2*), caspase 3 (*CASP3*), microtubule-associated protein 1 light chain 3 beta (*MAP1LC3B*), and autophagy-related 16 like 1 (*ATG16L1*) was tested in the present study. Glyceraldehyde-3-phosphate dehydrogenase (*GAPDH*) and (*RPSD*) RNA polymerase II subunit D were used as the housekeeping genes. Specific primers for target genes and housekeeping genes (Table 3) were synthesized by Sangon (China), and the application efficiency was then assessed. Quantitative PCR was conducted in an ABIPRISM 7500 Instrument (Applied Biosystems, USA) with ChamQ Universal SYBR qPCR Master Mix (#Q711, Vazyme, China). The relative gene expression of genes was calculated using the  $2^{-\Delta\Delta CT}$  method (36).

## 2.10 Western blot

The intestinal tissues were dissolved with RIPA lysis buffer (Solarbio, China) with the protease and phosphatase inhibitor (Roche, Switzerland). After centrifuging at 12000 g for 20 min at 4°C, the supernatants of the lysates were collected as the total proteins. The nuclear proteins of intestinal tissue were extracted using NE-PER<sup>TM</sup> Nuclear and Cytoplasmic Extraction Reagents (Thermo Fisher Scientific, USA), as the manufacturer's protocol showed. And then, the protein concentrations of the samples mentioned above were measured by the bicinchoninic acid (BCA) protein analysis kit (P0012, Beyotime, China). The

standardized samples were mixed with Omni-Easy<sup>TM</sup> Protein Sample Loading Buffer (EpiZyme, China). A total of 20 µg of protein was loaded and separated by sodium dodecyl sulfate-polyacrylamide gel electrophoresis. The proteins in the gel were transferred to a polyvinylidene difluoride (PVDF) membrane (Millipore, USA) for 1 h at 70 V, followed by membrane blocking at RT for 2 h with 5% non-fat milk (Sangon, China) in tris-buffered saline with Tween 20 (TBST). The membrane was incubated with primary antibodies overnight at 4°C and then washed three times for 5 min each with TBST. Next, the membrane was incubated with horseradish peroxidase (HRP)-conjugated secondary antibody (A0208, Beyotime, China) dissolved with 1% non-fat milk in the TBST for 1 h at RT. After washing with TBST 3 times for 5 min, the membrane was developed with enhanced chemiluminescence (Vazyme, China) according to the manufacturer's directions. The blots were recorded with an Odyssey Infrared Imaging System (Li-Cor Bioscience, USA). The following antibodies were used: antibodies against ASC (WL02462, Wanleibio, China), NF-κB p65 (8242, CST, USA), phos-IκBα<sup>ser32 ser36</sup> (2859, CST, USA), IκBα (WL01936, Wanleibio, China), Cleaved-caspase 3 (WL02117, Wanleibio, China), BCL2 (WL01556, Wanleibio, China), MAP1LC3B (AF5225, Beyotime, China), ATG16L1 (AF6252, Beyotime, China), Lamin B (AF1408, Beyotime, China), GAPDH (AB-P-R001, GoodHere, China). All the band intensities were quantified using ImageJ software (National Institutes of Health, USA). Respectively, the

TABLE 3 Primers used in quantitative real-time PCR (qRT-PCR).

Target gene	Forward primer (5'-3')	Reverse primer (5'-3')	GenBank no.
<i>MUC2</i>	ATGTGGAGTGTGTCGGCTT	AGACCTTGCACTGCATCTG	MF370857.1
<i>MUC18</i>	TTGTCCCTGACCAAGTGATG	ACAAAGCCTGTCCAAGATCG	JU370277.1
<i>CLDN4</i>	ATGTGGAGTGTGTCGGCTT	AGACCTTGCACTGCATCTG	MF370857.1
<i>TRIC</i>	GCCTACATCCACAAGACAACG	TCATTCAGCACTAATACAATCAC	KU238183.1
<i>JAM1</i>	CCAAGATGGACACCGGAAGT	CCTCCGGTGTGTTAGGTCACG	MT787206.1
<i>ZO1</i>	GAGTTTTCAGCTTCCGTGTT	AGAGAACCTGTCACTGATAGATGC	KU238184.1
<i>VDR</i>	CCACTTCAATGCCATGACC	TACTGCCCTAAAGAACCCT	XM_035644868.1
<i>VDRB</i>	TAATGGCAGTTGCACCATCACC	TCCTCTGCACTTCCTCGTCT	XM_035630011.1
<i>IL1B</i>	ATGGTGGCATTCTGTTC	CACITTTGGGTCGTCTTTG	AJ295836.2
<i>TNF</i>	GGACAGGGCTGGTACAACAC	TTCAATTAGTGCCACGACAAAGAG	AJ276709.1
<i>IL8</i>	GGAATTAATCCCTGGCAACTCT	ACCTCTTTGCGCTGAGTGT	XM_035638412.1
<i>IFNG</i>	GCTTTCCCGATCATCTTCTG	GGTTTCCAGATTCCCATTC	DQ400686.1
<i>TGFB1</i>	CTGCAGGACTGGCTCAAAGG	CATGGTCAGGATGTATGGTGGT	KU238187.1
<i>IL10</i>	TCGACGAGCTCAAGTCCGAT	CTGATCCAGCTCGCCCAT	XM_035632547.1
<i>CASP3</i>	TCGTTCTGTCTGTCTCTGTTGAG	GCTGTGGAGAAGGCGTAGAGG	XM_035637276.1
<i>BCL2</i>	GTGAACTGGGGCCGATTATC	CCATCCCCCGTTGTCCATAAT	XM_035631516.1
<i>BAX</i>	GCTCCAGAGGATGATAAATAAC	AAAGTAGAAGAGTGCAGACCA	XM_020094597.1
<i>MAP1LC3B</i>	GCACCCCAACAAGATCCCT	GATCTTGACCAGCTCGCTCA	XM_035642079.1
<i>ATG16L1</i>	GCAGATCACATTCTCCGCTCT	TGCCATCCAGCGAGACACC	XM_035621910.1
<i>GAPDH</i>	CAGTGTATGAAGCCAGCAGAG	GGTCGTATTGTCTCATTAACTC	AY008305.1
<i>RPSD</i>	AACACAGGAAGCAGCAGAAC	ACGGCAGTGATGGTCTCTC	DQ848899.1

densities of total protein bands and nuclear proteins were normalized to GAPDH or Lamin B, which served as internal controls.

## 2.11 Statistical analysis

Data were analyzed by one-way analysis of variance (ANOVA) using IBM SPSS Statistics for WINDOWS Version 22.0. Tukey's test was used to compare the means among individual treatments. Differences were regarded as significant when  $P < 0.05$ , and the results are presented as means  $\pm$  standard deviation (SD).

## 3 Results

### 3.1 VD<sub>3</sub> treatments *in vivo*

#### 3.1.1 Intestinal histology

H&E staining was used in the present study to study the effect of different VD<sub>3</sub> levels on the intestinal histology of turbot. The represented histological sections of the distal intestine are shown in Figure 1A. In the D<sub>0</sub> group, shortened mucosal fold, disordered goblet cells, and widened lamina propria were observed. However, the intestine of the D<sub>1</sub> and D<sub>2</sub> groups showed lengthened mucosal fold, well disturbing goblet cells, and reduced thickness of the lamina propria.

#### 3.1.2 Intestine-related enzyme activities *in vivo*

The activities of ALP, ACP, and LYZ were tested in the present study to reflect the intestinal immune status of turbot in different groups. Compared with the D<sub>0</sub> group, the D<sub>1</sub> and D<sub>2</sub> diets could significantly enhance the activities of ALP, ACP, and LYZ in the intestine of turbot ( $P < 0.05$ ) (Figure 1B).

#### 3.1.3 Mucins and tight junction proteins *in vivo*

Four intestinal tight junction proteins (*CLD4*, *TRIC*, *JAM1*, and *ZO1*) and two Mucins (*MUC2* and *MUC18*) gene expressions were analyzed in the present study. Compared with the D<sub>0</sub> diet, the D<sub>1</sub> diet significantly elevated the gene expression of *CLD4*, *TRIC*, and *ZO1* in the intestine ( $P < 0.05$ ), whereas the D<sub>2</sub> Diet prominently increased *TRIC* and *ZO1* mRNA levels ( $P < 0.05$ ) (Figure 1C). Compared with the D<sub>0</sub> diet, the D<sub>2</sub> diet significantly decreased the gene expression of *MUC2* in the intestine ( $P < 0.05$ ) (Figure 1C).

#### 3.1.4 VDRs and inflammation-related parameters *in vivo*

The gene expression of VDRs (*VDRA* & *B*), pro-inflammatory cytokines (*IL1B*, *IL8*, *TNF*, and *IFNG*), and anti-

inflammatory cytokines (*TGFB1* and *IL10*) was tested in the present study to indicate the intestinal inflammatory status. Compared with the D<sub>0</sub> diet, the D<sub>1</sub> diet significantly ( $P < 0.05$ ) suppressed the expression of pro-inflammatory cytokines (*IL1B*, *IL8*, *TNF*, and *IFNG*) but significantly ( $P < 0.05$ ) increased the expression of VDRs (*VDRA* and *VDRB*); D<sub>2</sub> diet markedly increased the expression of *VDRA* and *VDRB*, as well as the anti-inflammatory cytokines (*TGFB1* and *IL10*) ( $P < 0.05$ ) (Figures 1D, E).

And the protein level of NF- $\kappa$ B signaling pathway-related molecules (ASC, the ratio of phos-I $\kappa$ B $\alpha$ <sup>ser32 ser36</sup>/I $\kappa$ B $\alpha$  and intranuclear NF- $\kappa$ B p65) was tested in this study. Total ASC, the ratio of phos-I $\kappa$ B $\alpha$ <sup>ser32 ser36</sup>/I $\kappa$ B $\alpha$  and intranuclear NF- $\kappa$ B p65 in the intestine were significantly down-regulated by dietary VD<sub>3</sub> ( $P < 0.05$ ) (Figure 1J).

#### 3.1.5 Apoptosis-related parameters *in vivo*

DNA fragmentation could reflect the apoptosis level of intestine tissues. The DNA laddering of the three groups is shown in Figure 1G. The relative density of 180 to 200 bp DNA band was significantly ( $P < 0.05$ ) lower in the D<sub>1</sub> and D<sub>2</sub> groups compared with that in the D<sub>0</sub> groups (Figure 1H).

The gene expression of apoptosis-related genes (*CASP3*, *BAX*, and *BCL2*) was analyzed in the present study. The results of apoptosis-related gene expression showed that D<sub>1</sub> and D<sub>2</sub> diets significantly ( $P < 0.05$ ) reduced the gene expression of *CASP3* and *BAX* but remarkably ( $P < 0.05$ ) raised the gene expression of *BCL2* (Figure 1F).

The protein expression of apoptosis-related proteins (*CASP3* and *BCL2*) was also analyzed. The western blot results showed that both the D<sub>1</sub> and D<sub>2</sub> diets significantly ( $P < 0.05$ ) suppressed the expression of *CASP3* but increased the expression of *BCL2* considerably ( $P < 0.05$ ) (Figure 1I, K).

#### 3.1.6 Autophagy-related parameters *in vivo*

The gene and protein expression of autophagy-related genes (*ATG16L1* and *MAP1LC3B*) were analyzed in the present study. Dietary VD<sub>3</sub> significantly ( $P < 0.05$ ) elevated both the protein and mRNA expression of *ATG16L1* and *MAP1LC3B* (Figures 1F, I, K).

### 3.2 VD<sub>3</sub> treatments *in vitro*

#### 3.2.1 Tight junctions *in vitro*

Compared with the 0 nM 1,25(OH)<sub>2</sub>D<sub>3</sub> supplementation in intestinal epithelial cell *in vitro*, 1 nM 1,25(OH)<sub>2</sub>D<sub>3</sub> significantly ( $P < 0.05$ ) increased the gene expression of *ZO1*, 10 nM greatly ( $P < 0.05$ ) increased the expression of *CLD4* and *JAM1*, and 50nM remarkably ( $P < 0.05$ ) increased the expression of *JAM1* (Figure 2A).

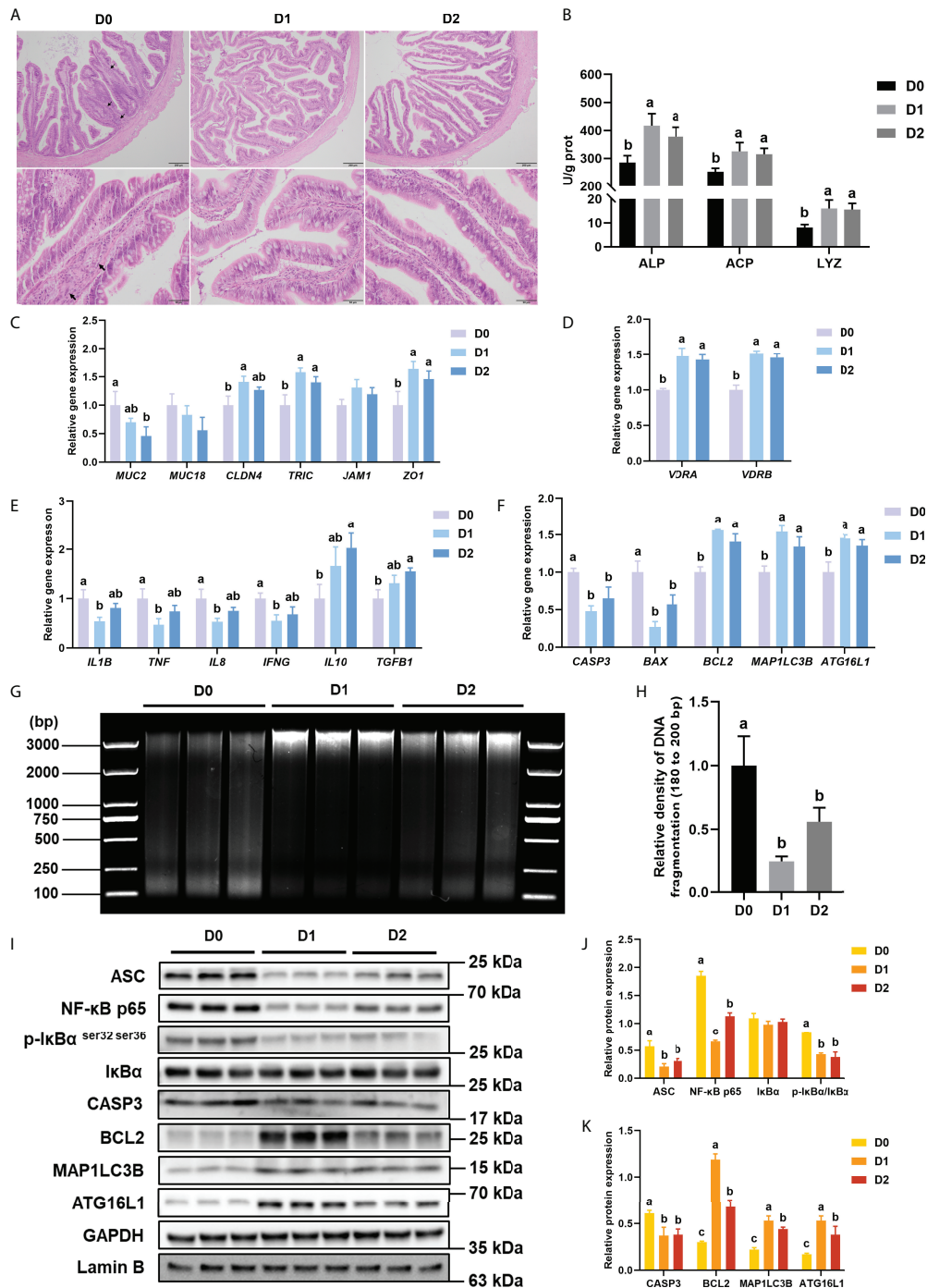


FIGURE 1

Inflammation, apoptosis, and autophagy of intestine with  $VD_3$  treatments *in vivo*. (A) H&E staining of intestine (Black bars, 200 μm or 50 μm), Black arrows indicate widening of the intestinal lamina propria. (B) Alkaline phosphatase, acid phosphatase activities, and lysozyme activities. (C) The relative mRNA expression level of *MUC2*, *MUC18*, *CLDN4*, *TRIC*, *JAM1*, and *ZO1*. (D) The relative mRNA expression level of *VDRα* & *B*. (E) The mRNA expression levels of *IL1B*, *TNF*, *IL8*, *IFNG*, *TGFB1*, and *IL10*. (F) The mRNA expression levels of *CASP3*, *BCL2*, *BAX*, *MAP1LC3B*, and *ATG16L1*. (G, H) DNA fragmentation and quantification of the density of the 180 to 200 bp DNA band. (I–K) The level of ASC, intranuclear NF-κB p65, total IκB and phosphorylated IκB, CASP3, BCL2, MAP1LC3B, and ATG16L1 were analyzed and quantitated by western blot. The blots of ASC, IκBα, p-IκBα<sub>ser32 ser36</sub>, CASP3, BCL2, MAP1LC3B, and ATG16L1 were used for GAPDH loading control, while the blot of NF-κB p65 was used for Lamin B loading control. Error bars of columns denote SD (n = 3), and columns with different letters above them are significantly different (P < 0.05).

### 3.2.2 VDRs and inflammation-related parameters *in vitro*

With the increase of 1,25(OH)<sub>2</sub>D<sub>3</sub> concentration in the culture medium, the expression of VDRA&B increased significantly ( $P < 0.05$ ) and reached the peak at the concentration of 50 nM 1,25(OH)<sub>2</sub>D<sub>3</sub> (Figure 2B). Compared with the 0 nM group, the mRNA level of *IL1B*, *TNF*, and *IFNG* was considerably decreased by the addition of 1,25(OH)<sub>2</sub>D<sub>3</sub> ( $P < 0.05$ ), whereas the gene expression of *IL10* was significantly ( $P < 0.05$ ) increased by the addition of 1,25(OH)<sub>2</sub>D<sub>3</sub> (Figure 2C). The treatments of 1,25(OH)<sub>2</sub>D<sub>3</sub> significantly ( $P < 0.05$ ) suppressed the expression of ASC, phos-IκB<sup>ser 32 ser36</sup>/IκB, and intranuclear NF-κB p65 (Figure 2G, H).

### 3.2.3 Apoptosis-related parameters *in vitro*

The TUNEL assay was conducted to test the apoptosis level of primary intestinal epithelial cells. DAPI stained both apoptotic and non-apoptotic cells blue, and only apoptotic nuclei had red fluorescence localized by TMR-5-dUTP incorporation. The TUNEL assay of cell climbing slides is shown in Figure 2E. Under the excitation of ultraviolet light, the nuclei stained by DAPI are blue, and the positive apoptotic nuclei are red. 1,25(OH)<sub>2</sub>D<sub>3</sub> obviously reduced the fluorescence intensity of positive apoptotic nuclei.

With the increasing addition of 1,25(OH)<sub>2</sub>D<sub>3</sub> in the medium, the gene expression of *CASP3* and *BAX* was significantly ( $P < 0.05$ ) decreased, while the *BCL2* expression was remarkably ( $P < 0.05$ ) enhanced (Figure 2D).

The treatment of 1,25(OH)<sub>2</sub>D<sub>3</sub> prominently ( $P < 0.05$ ) reduced the protein expression of *CASP3* but significantly ( $P < 0.05$ ) raised the protein expression of *BCL2* (Figure 2G, I).

### 3.2.4 Autophagy-related parameters *in vitro*

As shown in Figure 2D, the highest gene expression of *ATG16L1* was observed in treatment with 1 nM 1,25(OH)<sub>2</sub>D<sub>3</sub> ( $P < 0.05$ ). The treatments of 1,25(OH)<sub>2</sub>D<sub>3</sub> significantly ( $P < 0.05$ ) enhanced the protein expression of *MAP1LC3B* and *ATG16L1* (Figure 2I).

Immunofluorescence was conducted to analyze the intracellular localization of *MAP1LC3B*. Following the immunofluorescence results of cell climbing slides (DAPI, blue; *MAP1LC3B* fluorescence, red), the additions of 1,25(OH)<sub>2</sub>D<sub>3</sub> in the cell promoted the fluorescence of *MAP1LC3B* (Figure 2F, G).

## 3.3 RNA interference of VDR *in vivo*

### 3.3.1 Efficiencies of VDR siRNAs *in vivo*

As shown in Figure 3A, the result indicated that the VDRA siRNA 3 and VDRB siRNA1 were the most efficient ( $P < 0.05$ ) duplex for knocking down VDRA&B expression in the intestine

of turbot (about 50% and 70%, respectively), which were selected for the following experiments.

### 3.3.2 Inflammation-related parameters after VDR RNAi *in vivo*

Compared with the PBS group, the LPS injection significantly ( $P < 0.05$ ) enhanced the gene expression of pro-inflammatory cytokines (*IL1B* and *IL8*) but prominently ( $P < 0.05$ ) suppressed the mRNA level of anti-inflammatory cytokines (*IL10* and *TGFB1*) in the intestine of turbot. Compared with NC siRNA+LPS group, the gene expression of *IL1B* significantly ( $P < 0.05$ ) increased, and *IL10* and *TGFB1* significantly ( $P < 0.05$ ) decreased in the siVDR treated groups (Figure 3B). The results of western blot showed that the knockdown of VDRA&B remarkably ( $P < 0.05$ ) activated the NF-κB signalling in terms of a significant ( $P < 0.05$ ) increase of ASC, intranuclear NF-κB p65, and phos-IκB<sup>ser 32 ser36</sup>/IκB (Figure 3D, E).

### 3.3.3 Apoptosis-related parameters after VDR RNAi *in vivo*

The gene expression of *CASP3* and *BAX* after LPS stimulation was significantly higher ( $P < 0.05$ ) than the expression in the PBS group. The VDRA&B knockdown significantly ( $P < 0.05$ ) induced the gene expression of *CASP3* and *BAX* compared to the NC siRNA when injected by LPS (Figure 3C). A similar result was also observed in western blot analysis that the protein expression of *BCL2* was significantly ( $P < 0.05$ ) lower in the VDRA siRNA 3+LPS and VDRB siRNA 1+LPS than that in the NC siRNA+LPS group (Figure 3D, F).

### 3.3.4 Autophagy-related parameters after VDR RNAi *in vivo*

The injection of LPS prominently ( $P < 0.05$ ) reduced the gene expression of *MAP1LC3B* and *ATG16L1* in the intestine of the turbot. Compared with the NC siRNA+LPS group, the knockdown of VDRA&B led to a significant ( $P < 0.05$ ) reduction of gene and protein expression of *MAP1LC3B* and *ATG16L1* (Figures 3C, D, F).

## 4 Discussion

According to the previous diagnostic criteria of enteritis in Atlantic salmon (*Salmo salar* L.) (37) and turbot (38), typical intestinal enteritis histomorphology was observed in the VD<sub>3</sub> deficiency group in terms of shortened mucosal fold, disordered goblet cells, and widened lamina propria. Besides, a reduced expression of tight junction proteins, decreased mucin secretion, overexpression of pro-inflammatory cytokines, and suppressed immune response were also involved in the pathological process

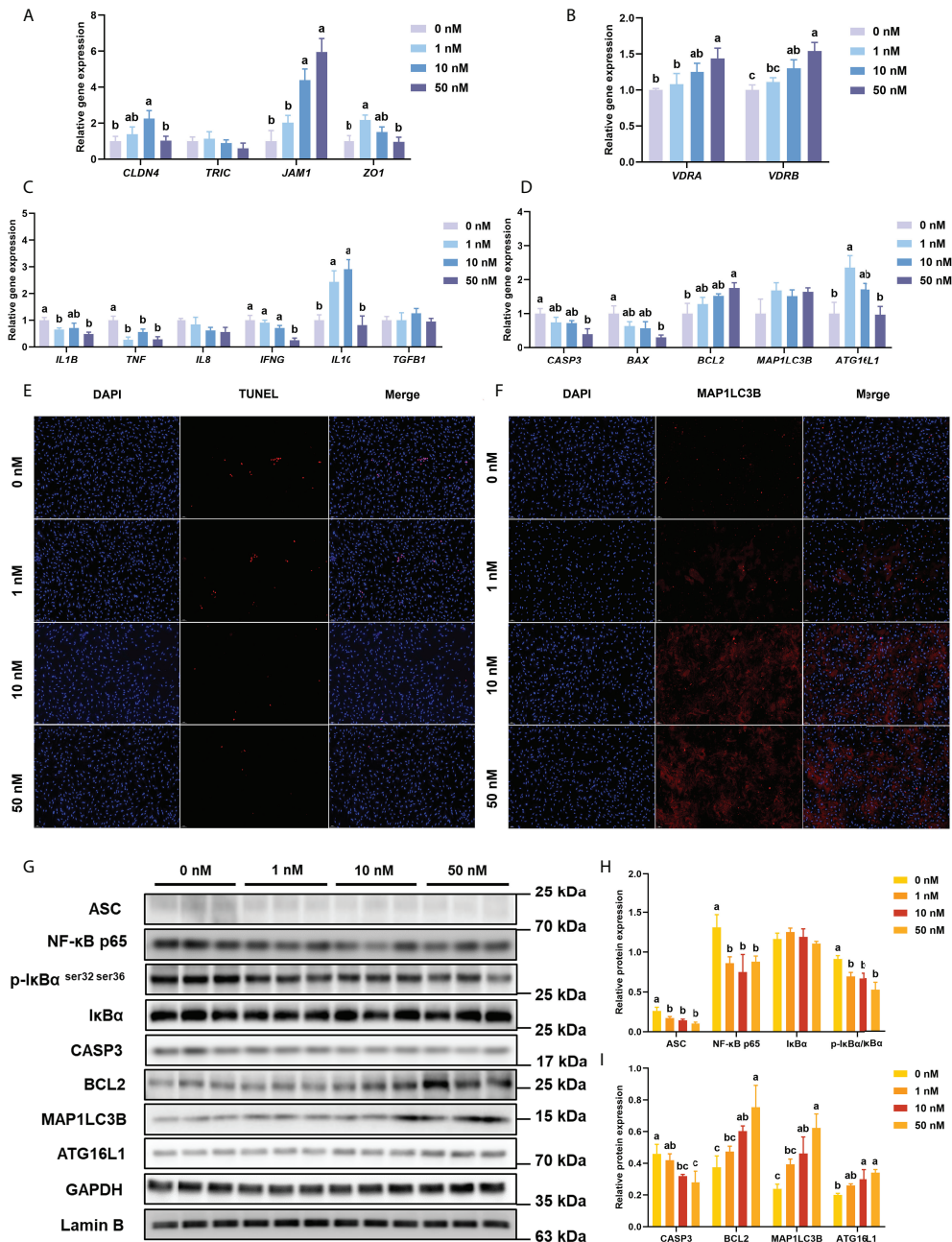


FIGURE 2

Inflammation, apoptosis, and autophagy of intestinal epithelial cells with  $VD_3$  treatments *in vitro*. (A) The relative mRNA expression level of *CLDN4*, *TRIC*, *JAM1*, and *ZO1*. (B) The relative mRNA expression level of *VDR A/B*. (C) The mRNA expression levels of *IL1B*, *TNF*, *IL8*, *IFNG*, *TGFB1*, and *IL10*. (D) The mRNA expression levels of *CASP3*, *BCL2*, *BAX*, *MAP1LC3B*, and *ATG16L1*. (E) Confocal images of TUNEL assay (White bars, 50  $\mu$ m). (F) Confocal images of MAP1LC3B fluorescence (White bars, 50  $\mu$ m). (G-I) The level of ASC, intranuclear NF- $\kappa$ B p65, total I $\kappa$ B and phosphorylated I $\kappa$ B, CASP3, BCL2, MAP1LC3B, and ATG16L1 were analyzed and quantitated by western blot. The blots of ASC, I $\kappa$ B $\alpha$ , p-I $\kappa$ B $\alpha$ <sup>ser32/ser36</sup>, CASP3, BCL2, MAP1LC3B, and ATG16L1 were used for GAPDH loading control, while the blot of NF- $\kappa$ B p65 was used for Lamin B loading control. Error bars of columns denote SD (n = 3), and columns with different letters above them are significantly different ( $P < 0.05$ ).

of enteritis in fish (3, 4, 6, 39). In the present study, suppressed secretion of intestinal mucus and lower expression of tight junction protein led to the intestinal mucosal barrier dysfunction in turbot, which was also observed *in vitro*

(reduction in the gene expression of tight junction proteins). Moreover, the mRNA levels of pro-inflammatory and anti-inflammatory cytokines in  $VD_3$  deficiency treatment were significantly enhanced or suppressed *in vivo* and *in vitro*,

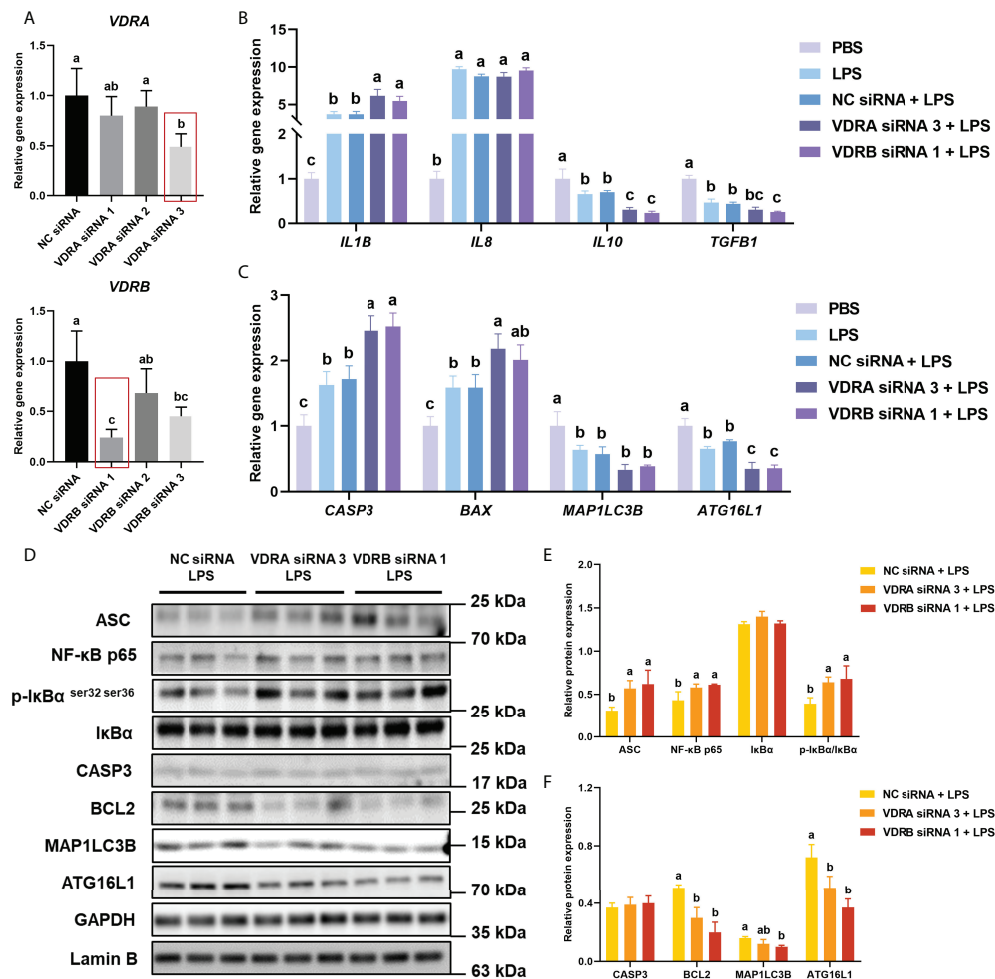


FIGURE 3

VDR knockdown *in vivo* on inflammation, apoptosis, and autophagy in the intestine. (A) The relative mRNA expression level of VDRA and VDRB in the intestine treated with VDRA and VDRB siRNAs. (B) The mRNA expression levels of *IL1B*, *IL8*, *TGFB1*, and *IL10*. (C) The mRNA expression levels of *CASP3*, *BCL2*, *BAX*, *MAP1LC3B*, and *ATG16L1*. (D–F) The level of ASC, intranuclear NF-κB p65, total IκB and phosphorylated IκB, *CASP3*, *BCL2*, *MAP1LC3B*, and *ATG16L1* were analyzed and quantitated by western blot. The blots of ASC, IκBα, p-IκBα<sup>ser32/ser36</sup>, *CASP3*, *BCL2*, *MAP1LC3B*, and *ATG16L1* were used for GAPDH loading control, while the blot of NF-κB p65 was used for Lamin B loading control. Error bars of columns denote SD (n = 3), and columns with different letters above them are significantly different ( $P < 0.05$ ).

respectively. In addition, the *in vivo* results showed that VD<sub>3</sub> deficiency contributed to the reduced intestinal immune-related enzyme activities of ACP, ALP, and LYZ activities. These results showed that the deficiency of VD<sub>3</sub> in diet could induce intestinal enteritis of turbot, which was consistent with the previous studies that diets with sufficient VD<sub>3</sub> are the basis for maintaining intestinal immune function, and VD<sub>3</sub> deficiency provoked an intestinal inflammatory response in European sea bass (*Dicentrarchus labrax* L.) and Chinese mitten crabs (5, 8).

In the present study, VD<sub>3</sub> deficiency in diet activated the NF-κB signalling pathway of turbot by blocking NF-κB nuclear translocation and reducing IκBα phosphorylation. Generally, activation of NF-κB signalling activates the inflammasome by promoting the expression of the inflammasome adaptor ASC,

which may also lead to increased expression and secretion of interleukins (40). In the present study, dietary administration of VD<sub>3</sub> suppressed intestinal inflammation by down-regulating the NF-κB/inflammasome signalling. In male Sprague–Dawley rats, the treatment of VD<sub>3</sub> suppressed the exercise-induced muscle inflammation through the modulation of MAPK and NF-κB involved with VDR (41). The study in abalone (*Haliotis discus hannai*) also showed that VD<sub>3</sub> could inhibit inflammation by significantly decreasing the phosphorylation of IKK and IκB and further blocking nuclear translocation of NF-κB (32).

A steady accumulation of studies showed that apoptosis and autophagy are often regulated by similar pathways and usually cooperated in a balanced interplay or facilitated cellular destruction in a complementary fashion (42). Effects of VD<sub>3</sub>

on apoptosis are diverse in different studies because of the different experimental procedures, concentrations of VD<sub>3</sub>, and the species of animals. On the one hand, VD<sub>3</sub> could increase apoptosis in the treatment of cancer, obesity, and inflammatory bowel disease (43–45). On the other hand, studies in the murine showed that the exogenous VD<sub>3</sub> attenuated the cell apoptosis in LPS-induced lung injury and hippocampal apoptosis induced by kainic acid and pentylentetrazol (46, 47). DNA fragmentation assay is an apparent indicator of apoptosis, and one of the most distinctive characteristics is the 180 to 200 bp fragments (35). Under the inflamed circumstance in the intestine, diets with VD<sub>3</sub> supplementation prominently decreased the relative density of the DNA ladder, especially the 180 to 200 bp DNA band, indicating that dietary VD<sub>3</sub> could reduce the intestinal apoptosis of turbot in this study. Similarly, the TUNEL assay showed that VD<sub>3</sub> reduced the fluorescence intensity of positive apoptotic nuclei, indicating that the administration of VD<sub>3</sub> in turbot was crucial to ameliorate DNA damage in apoptosis. In the process of apoptosis activation, BCL2 blocked the release of cytochrome C by preventing the pores in the mitochondrial outer membrane formed by the combo of BAX and BCL2 Antagonist/Killer (BAK) proteins, which inhibited the activation of the caspases for dismantling the cell (48–52). In this study, VD<sub>3</sub> deficiency resulted in the higher expression of CASP3 and BAX, and the lower expression of BCL2. Similar results were also observed in the study on MCF-7 breast cancer cell line that the regulation of VD<sub>3</sub> on apoptosis was BAX and BCL2 depended (53). The present results indicated that intestinal apoptosis could be enhanced in response to the aggressive intestinal inflammation induced by VD<sub>3</sub> deficiency, and this process relied on activating BAX/BAK combo and inhibiting BCL2.

Autophagy within the epithelium controlled inflammation-induced apoptosis and barrier integrity to limit chronic intestinal inflammation (54). ATG16L1 contributed to the addition of lipid moieties to the ubiquitin-like molecule MAP1LC3B, which promoted autophagosome formation and function (55). The present results showed that VD<sub>3</sub> deficiency suppressed the expression of ATG16L1 and MAP1LC3B, and confocal images of MAP1LC3B fluorescence *in vitro* showed that the fluorescence reaction was significantly reduced without VD<sub>3</sub> stimulation. And the reduction of intestinal autophagy status could be alleviated by the addition of VD<sub>3</sub>. Taken these results together, VD<sub>3</sub> can suppress the activation of apoptosis but enhance autophagy in turbot. Moreover, the mutually exclusive cellular states of apoptosis and autophagy were also observed in abalone, in which dietary VD<sub>3</sub> can significantly increase the expression of autophagy-related proteins but decrease the expression of apoptosis-related proteins (32).

Previous studies in mammals demonstrated that the VDR was involved in the inhibition of NF- $\kappa$ B nuclear translocation, which

suppressed the expression of pro-inflammatory cytokines (56, 57). VDR also plays an important role in apoptosis. For example, the VDR/ERK signalling pathway inhibited the apoptotic cascade in hippocampal CA1 neurons of global cerebral ischemia rats (58). VDR can also inhibit high glucose-induced endothelial cell apoptosis by inhibiting oxidative stress (59). In addition, VDR may play a crucial role in vitamin D regulation of autophagy in hepatitis C virus viral infection (60). The current results showed that the gene expression of VDR was up-regulated by dietary VD<sub>3</sub>, and the knockdown of VDR in turbot aggravated the LPS-induced intestinal inflammatory response and apoptosis, while the reduced autophagy led by the VDR silencing was further declined. Thus, VD<sub>3</sub>/VDR is involved in alleviating the intestinal inflammatory response of turbot and maintaining the dynamic balance of apoptosis and autophagy.

## 5 Conclusion

The present study showed that VD<sub>3</sub> deficiency in diet could induce intestinal enteritis of turbot. The inflammatory response caused by VD<sub>3</sub> deficiency was regulated by the NF- $\kappa$ B/inflammasome pathway; interestingly, the regulation of VD<sub>3</sub> on intestinal inflammatory response may be related to intestinal epithelial cell apoptosis and autophagy, establishing an antagonism of apoptosis and autophagy. Further, the regulation of VD<sub>3</sub> on the inflammatory response, apoptosis, and autophagy was VDR-dependent. Besides, excessive VD<sub>3</sub> (4000 IU/kg) did not adversely impact turbot as in mammals, and further research relating to VD<sub>3</sub> metabolism is needed to explain these results.

## Data availability statement

The original contributions presented in the study are included in the article/[Supplementary Material](#). Further inquiries can be directed to the corresponding authors.

## Ethics statement

The animal study was reviewed and approved by Institutional Animal Care and Use Committee of the Ocean University of China.

## Author contribution

Conceptualization: ZC, DH, JD, and YZ; Methodology: ME, OJ, WZ, QA, KM, JD, and YZ; Formal analysis and investigation: ZC, DH, PY, and GL; Writing - original draft preparation: ZC; Writing - review and editing: ZC, DH, ME, OJ, WZ, QA, KM,

JD, and YZ; Funding acquisition: YZ; Supervision: JD and YZ. All authors contributed to the article and approved the submitted version.

## Funding

This work was supported by the National Natural Science Foundation of China (No. 31872577); the National Key R&D Program of China (2019YFD0900104); China Agriculture Research System (Grant No. CARS 47-G10). ZC appreciated the financial support from the China Scholarship Council by a State Scholarship Fund (No.201806330100).

## Conflict of interest

The authors declare that the research was conducted in the absence of any commercial or financial relationships that could be construed as a potential conflict of interest.

## References

- Abreu MT, Fukata M, Arditi M. TLR signaling in the gut in health and disease. *J Immunol* (2005) 174:4453–60. doi: 10.4049/jimmunol.174.8.4453
- König J, Wells J, Cani PD, García-Ródenas CL, Macdonald T, Mercenier A, et al. Human intestinal barrier function in health and disease. *Clin Trans Gastroenterol* (2016) 7:e196. doi: 10.1038/ctg.2016.54
- Chen Z, Liu Y, Li Y, Yang P, Hu H, Yu G, et al. Dietary arginine supplementation mitigates the soybean meal induced enteropathy in juvenile turbot, *Scophthalmus maximus* L. *Aquaculture Res* (2018) 49:1535–45. doi: 10.1111/are.13608
- Chen Z, Zhao S, Liu Y, Yang P, Ai Q, Zhang W, et al. Dietary citric acid supplementation alleviates soybean meal-induced intestinal oxidative damage and micro-ecological imbalance in juvenile turbot, *Scophthalmus maximus* L. *Aquaculture Res* (2018) 49:3804–16. doi: 10.1111/are.13847
- Liu S, Wang X, Bu X, Lin Z, Li E, Shi Q, et al. Impact of dietary vitamin D<sub>3</sub> supplementation on growth, molting, antioxidant capability, and immunity of juvenile Chinese mitten crabs (*Eriocheir sinensis*) by metabolites and vitamin D receptor. *J Agric Food Chem* (2021) 69:12794–806. doi: 10.1021/acs.jafc.1c04204
- Yu G, Liu Y, Ou W, Dai J, Ai Q, Zhang W, et al. The protective role of daidzein in intestinal health of turbot (*Scophthalmus maximus* L.) fed soybean meal-based diets. *Sci Rep* (2021) 11:1–13. doi: 10.1038/s41598-021-82866-1
- Fenwick JC. Effect of vitamin D<sub>3</sub> (cholecalciferol) on plasma calcium and intestinal 45calcium absorption in goldfish, *carassius auratus* L. *Can J Zool* (1984) 62:34–6. doi: 10.1139/z84-007
- Dioguardi M, Guardiola F, Vazzana M, Cuesta A, Esteban M, Cammarata M. Vitamin D<sub>3</sub> affects innate immune status of European sea bass (*Dicentrarchus labrax* L.). *Fish Physiol Biochem* (2017) 43:1161–74. doi: 10.1007/s10695-017-0362-3
- Takeuchi A, Okano T, Sayamoto M, Sawamura S, Kobayashi T, Motosugi M, et al. Tissue distribution of 7-dehydrocholesterol, vitamin D<sub>3</sub> and 25-hydroxyvitamin D<sub>3</sub> in several species of fishes. *J Nutr Sci Vitaminol* (1986) 32:13–22. doi: 10.3177/jnsv.32.13
- Kennel KA, Drake MT, Hurley DL. Vitamin D deficiency in adults: when to test and how to treat. *Amsterdam: Elsevier* (2010) 85(8):752–8. doi: 10.4065/mcp.2010.0138

The reviewer SZ declared a shared affiliation with authors GL and JD to the editor at the time of review.

## Publisher's note

All claims expressed in this article are solely those of the authors and do not necessarily represent those of their affiliated organizations, or those of the publisher, the editors and the reviewers. Any product that may be evaluated in this article, or claim that may be made by its manufacturer, is not guaranteed or endorsed by the publisher.

## Supplementary material

The Supplementary Material for this article can be found online at: <https://www.frontiersin.org/articles/10.3389/fimmu.2022.986593/full#supplementary-material>

- Ardesia M, Ferlazzo G, Fries W. Vitamin D and inflammatory bowel disease. *BioMed Res Int* (2015) 2015:470805. doi: 10.1155/2015/470805
- Barbáchano A, Fernández-Barral A, Ferrer-Mayorga G, Costales-Carrera A, Larriba MJ, Muñoz A. The endocrine vitamin D system in the gut. *Mol Cell Endocrinol* (2017) 453:79–87. doi: 10.1016/j.mce.2016.11.028
- Kong J, Zhang Z, Musch MW, Ning G, Sun J, Hart J, et al. Novel role of the vitamin D receptor in maintaining the integrity of the intestinal mucosal barrier. *Am J Physiology-Gastrointestinal Liver Physiol* (2008) 294:G208–16. doi: 10.1152/ajpgi.00398.2007
- Christakos S, Dhawan P, Ajibade D, Benn BS, Feng J, Joshi SS. Mechanisms involved in vitamin D mediated intestinal calcium absorption and in non-classical actions of vitamin D. *J Steroid Biochem Mol Biol* (2010) 121:183–7. doi: 10.1016/j.jsbmb.2010.03.005
- Zhang YG, Wu S, Sun J. Vitamin D, vitamin D receptor and tissue barriers. *Tissue Barriers* (2013) 1:e23118. doi: 10.4161/tisb.23118
- Koshiji M, Adachi Y, Sogo S, Taketani S, Oyaizu N, Than S, et al. Apoptosis of colorectal adenocarcinoma (COLO 201) by tumour necrosis factor-alpha (TNF- $\alpha$ ) and/or interferon-gamma (IFN- $\gamma$ ), resulting from down-modulation of bcl-2 expression. *Clin Exp Immunol* (1998) 111:211–8. doi: 10.1046/j.1365-2249.1998.00460.x
- Croituru K, Zhou P. T-cell-induced mucosal damage in the intestine. *Curr Opin Gastroenterol* (2004) 20:581–6. doi: 10.1097/00001574-200411000-00013
- Edelblum KL, Yan F, Yamaoka T, Polk BD. Regulation of apoptosis during homeostasis and disease in the intestinal epithelium. *Inflammatory Bowel Dis* (2006) 12:413–24. doi: 10.1097/01.MIB.0000217334.30689.3e
- Saitoh T, Fujita N, Jang MH, Uematsu S, Yang B-G, Satoh T, et al. Loss of the autophagy protein Atg16L1 enhances endotoxin-induced IL-1 $\beta$  production. *Nature* (2008) 456:264–8. doi: 10.1038/nature07383
- Cabrera S, Fernández ÁF, Mariño G, Aguirre A, Suárez MF, Español Y, et al. ATG4B/autophagin-1 regulates intestinal homeostasis and protects mice from experimental colitis. *Autophagy* (2013) 9:1188–200. doi: 10.4161/auto.24797
- Tsuboi K, Nishitani M, Takakura A, Imai Y, Komatsu M, Kawashima H. Autophagy protects against colitis by the maintenance of normal gut microflora

- and secretion of mucus. *J Biol Chem* (2015) 290:20511–26. doi: 10.1074/jbc.M114.632257
22. Zhang H, Zheng L, Mcgovern DP, Hamill AM, Ichikawa R, Kanazawa Y, et al. Myeloid ATG16L1 facilitates host–bacteria interactions in maintaining intestinal homeostasis. *J Immunol* (2017) 198:2133–46. doi: 10.4049/jimmunol.1601293
23. Massey D, Bredin F, Parkes M. Use of sirolimus (rapamycin) to treat refractory crohn's disease. *Gut* (2008) 57:1294–6. doi: 10.1136/gut.2008.157297
24. Hu S, Chen M, Wang Y, Wang Z, Pei Y, Fan R, et al. mTOR inhibition attenuates dextran sulfate sodium-induced colitis by suppressing T cell proliferation and balancing TH1/TH17/Treg profile. *PLoS One* (2016) 11: e0154564. doi: 10.1371/journal.pone.0159758
25. Macias-Ceja DC, Cosin-Roger J, Ortiz-Masiá D, Salvador P, Hernández C, Esplugues JV, et al. Stimulation of autophagy prevents intestinal mucosal inflammation and ameliorates murine colitis. *Br J Pharmacol* (2017) 174:2501–11. doi: 10.1111/bph.13860
26. Díaz GD, Paraskeva C, Thomas MG, Binderup L, Hague A. Apoptosis is induced by the active metabolite of vitamin D<sub>3</sub> and its analogue EB1089 in colorectal adenoma and carcinoma cells: possible implications for prevention and therapy. *Cancer Res* (2000) 60:2304–12.
27. Lu R, Zhang YG, Xia Y, Sun J. Imbalance of autophagy and apoptosis in intestinal epithelium lacking the vitamin D receptor. *FASEB J* (2019) 33:11845–56. doi: 10.1096/fj.201900727R
28. Varghese JE, Shanmugam V, Rengarajan RL, Meyyazhagan A, Arumugam VA, Al-Misned FA, et al. Role of vitamin D<sub>3</sub> on apoptosis and inflammatory-associated gene in colorectal cancer: An *in vitro* approach. *J King Saud University-Science* (2020) 32:2786–9. doi: 10.1016/j.jksus.2020.06.015
29. Rubinstein AD, Kimchi A. Life in the balance—a mechanistic view of the crosstalk between autophagy and apoptosis. *J Cell Sci* (2012) 125:5259–68. doi: 10.1242/jcs.115865
30. Murthy A, Li Y, Peng I, Reichelt M, Katakam AK, Noubade R, et al. A crohn's disease variant in Atg16L1 enhances its degradation by caspase 3. *Nature* (2014) 506:456–62. doi: 10.1038/nature13044
31. Wu S, Zhang Y-G, Lu R, Xia Y, Zhou D, Petrof EO, et al. Intestinal epithelial vitamin D receptor deletion leads to defective autophagy in colitis. *Gut* (2015) 64:1082–94. doi: 10.2353/ajpath.2010.090998
32. Huang D, Guo Y, Li X, Pan M, Liu J, Zhang W, et al. Vitamin D<sub>3</sub>/VDR inhibits inflammation through NF-κB pathway accompanied by resisting apoptosis and inducing autophagy in abalone *Haliotis discus hannai*. *Cell Biol Toxicol* (2021) 1–22. doi: 10.1007/s10565-021-09647-4
33. Horvli O, Lie Ø. Determination of vitamin D<sub>3</sub> in fish meals by HPLC. *Fiskeridirektoratets Skrifter Serie Ernæring* (1994) 6:163–75.
34. Yu G, Ou W, Ai Q, Zhang W, Mai K, Zhang Y. *In vitro* study of sodium butyrate on soyasaponin challenged intestinal epithelial cells of turbot (*Scophthalmus maximus* L.) refer to inflammation, apoptosis and antioxidant enzymes. *Fish Shellfish Immunol Rep* (2021) 2:100031. doi: 10.1016/j.fsirep.2021.100031
35. Yuan Z, Feng L, Jiang W, Wu P, Liu Y, Kuang S, et al. Dietary choline deficiency aggravated the intestinal apoptosis in association with the MAPK signalling pathways of juvenile grass carp (*Ctenopharyngodon idella*). *Aquaculture* (2021) 532:736046. doi: 10.1016/j.aquaculture.2020.736046
36. Livak KJ, Schmittgen TD. Analysis of relative gene expression data using real-time quantitative PCR and the 2<sup>-ΔΔCT</sup> method. *Methods* (2001) 25:402–8. doi: 10.1006/meth.2001.1262
37. Krogdahl Å, Bakke-Mckeller A, Baeverfjord G. Effects of graded levels of standard soybean meal on intestinal structure, mucosal enzyme activities, and pancreatic response in Atlantic salmon (*Salmo salar* L.). *Aquaculture Nutr* (2003) 9:361–71. doi: 10.1046/j.1365-2095.2003.00264.x
38. Liu Y, Chen Z, Dai J, Yang P, Xu W, Ai Q, et al. Sodium butyrate supplementation in high-soybean meal diets for turbot (*Scophthalmus maximus* L.): effects on inflammatory status, mucosal barriers and microbiota in the intestine. *Fish Shellfish Immunol* (2019) 88:65–75. doi: 10.1016/j.fsi.2019.02.064
39. Liu Y, Chen Z, Dai J, Yang P, Hu H, Ai Q, et al. The protective role of glutamine on enteropathy induced by high dose of soybean meal in turbot, *Scophthalmus maximus* L. *Aquaculture* (2018) 497:510–9. doi: 10.1016/j.aquaculture.2018.08.021
40. Gross O, Poeck H, Bscheider M, Dostert C, Hanneschläger N, Endres S, et al. Syk kinase signalling couples to the Nlrp3 inflammasome for anti-fungal host defence. *Nature* (2009) 459:433–6. doi: 10.1038/nature07965
41. Choi M, Park H, Cho S, Lee M. Vitamin D<sub>3</sub> supplementation modulates inflammatory responses from the muscle damage induced by high-intensity exercise in SD rats. *Cytokine* (2013) 63:27–35. doi: 10.1016/j.cyto.2013.03.018
42. Nikolettou V, Markaki M, Palikaras K, Tavernarakis N. Crosstalk between apoptosis, necrosis and autophagy. *Biochim Biophys Acta (BBA)-Molecular Cell Res* (2013) 1833:3448–59. doi: 10.1016/j.bbamcr.2013.06.001
43. Martinesi M, Treves C, D'Albasio G, Bagnoli S, Bonanomi AG, Stio M. Vitamin D derivatives induce apoptosis and downregulate ICAM-1 levels in peripheral blood mononuclear cells of inflammatory bowel disease patients. *Inflammatory Bowel Dis* (2008) 14:597–604. doi: 10.1002/ibd.20354
44. Sergeev IN. Vitamin D-mediated apoptosis in cancer and obesity. *Hormone Mol Biol Clin Invest* (2014) 20:43–9. doi: 10.1515/hmbci-2014-0035
45. Sergeev IN. Vitamin D status and vitamin D-dependent apoptosis in obesity. *Nutrients* (2020) 12:1392. doi: 10.3390/nu12051392
46. Şahin S, Gürgeç SG, Yazar U, İnce İ, Kamaşak T, Arslan EA, et al. Vitamin D protects against hippocampal apoptosis related with seizures induced by kainic acid and pentylentetrazol in rats. *Epilepsy Res* (2019) 149:107–16. doi: 10.1016/j.eplepsyres.2018.12.005
47. Zheng S, Yang J, Hu X, Li M, Wang Q, Dancer RC, et al. Vitamin D attenuates lung injury via stimulating epithelial repair, reducing epithelial cell apoptosis and inhibits TGF-β induced epithelial to mesenchymal transition. *Biochem Pharmacol* (2020) 177:113955. doi: 10.1016/j.bcp.2020.113955
48. Goldstein JC, Waterhouse NJ, Juin P, Evan GI, Green DR. The coordinate release of cytochrome c during apoptosis is rapid, complete and kinetically invariant. *Nat Cell Biol* (2000) 2:156–62. doi: 10.1038/35004029
49. Shi Y. Mechanisms of caspase activation and inhibition during apoptosis. *Mol Cell* (2002) 9:459–70. doi: 10.1016/S1097-2765(02)00482-3
50. Elmore S. Apoptosis: a review of programmed cell death. *Toxicologic Pathol* (2007) 35:495–516. doi: 10.1080/01926230701320337
51. D'arcy MS. Cell death: a review of the major forms of apoptosis, necrosis and autophagy. *Cell Biol Int* (2019) 43:582–92. doi: 10.1002/cbin.11137
52. Lv F, Qi F, Zhang Z, Wen M, Kale J, Piai A, et al. An amphipathic bax core dimer forms part of the apoptotic pore wall in the mitochondrial membrane. *EMBO J* (2014) 40(14):e106438. doi: 10.15252/embj.2020106438
53. Alamro AA, Al-Malky MM, Ansari MG, Amer OE, Alnaami AM, Hussain SD, et al. The effects of melatonin and vitamin D<sub>3</sub> on the gene expression of BCL-2 and BAX in MCF-7 breast cancer cell line. *J King Saud University-Science* (2021) 33:101287. doi: 10.1016/j.jksus.2020.101287
54. Pott J, Kabat AM, Maloy KJ. Intestinal epithelial cell autophagy is required to protect against TNF-induced apoptosis during chronic colitis in mice. *Cell Host Microbe* (2018) 23:191–202. doi: 10.1016/j.chom.2017.12.017
55. Grizotte-Lake M, Vaishnav S. Autophagy: suicide prevention hotline for the gut epithelium. *Cell Host Microbe* (2018) 23:147–8. doi: 10.1016/j.chom.2018.01.015
56. Wu S, Liao AP, Xia Y, Li YC, Li J-D, Sartor RB, et al. Vitamin D receptor negatively regulates bacterial-stimulated NF-κB activity in intestine. *Am J Pathol* (2010) 177:686–97. doi: 10.2353/ajpath.2010.090998
57. Chen Y, Zhang J, Ge X, Du J, Deb DK, Li YC. Vitamin D receptor inhibits nuclear factor κB activation by interacting with IκB kinase β protein. *J Biol Chem* (2013) 288:19450–8. doi: 10.1074/jbc.M113.467670
58. Guo X, Yuan J, Wang J, Cui C, Jiang P. Calcitriol alleviates global cerebral ischemia-induced cognitive impairment by reducing apoptosis regulated by VDR/ERK signaling pathway in rat hippocampus. *Brain Res* (2019) 1724:146430. doi: 10.1016/j.brainres.2019.146430
59. Zhang M, Lin L, Xu C, Chai D, Peng F, Lin J. VDR agonist prevents diabetic endothelial dysfunction through inhibition of prolyl isomerase-1-mediated mitochondrial oxidative stress and inflammation. *Oxid Med Cell Longevity* (2018) 2018:1714896. doi: 10.1155/2018/1714896
60. Abdel-Mohsen MA, El-Braky AA, Ghazal AAE, Shamseya MM. Autophagy, apoptosis, vitamin D, and vitamin D receptor in hepatocellular carcinoma associated with hepatitis c virus. *Medicine* (2018) 97(12):e0172. doi: 10.1097/md.00000000000010172